

VALIDATION OF A MULTISCALE COUPLING ALGORITHM BY EXPERIMENTAL TESTS IN TALL-3D FACILITY

Antonio Cervone¹, Andrea Chierici^{2*}, Leonardo Chirco², Roberto Da Vià²
and Sandro Manservigi²

¹ ENEA, Via Martiri di Monte Sole, 4, 40129 Bologna, Italy

² University of Bologna - DIN, Via dei Colli 16, 40136 Bologna (BO), Italy

*e-mail: andrea.chierici4@unibo.it

Key words: Multiscale Methods, Coupling Codes, Thermo-Hydraulics, Nuclear Systems

Abstract. A multiscale coupling algorithm has been developed and validated through the numerical simulation of the thermal hydraulic behavior of an unprotected loss of flow in the experimental TALL-3D facility. During the loss of flow the system goes from forced to natural circulation flow. TALL-3D is a liquid Lead Bismuth Eutectic (LBE) loop, with an oil-cooled secondary loop, developed according to the requirements for the experimental data for validation of coupled CFD and system codes. In this work we perform the coupling between the multigrid finite element code FEMuS and a system code, by using a defective coupling algorithm of a one-dimensional circuit and a three-dimensional test section with overlapping meshes. A multiscale and multiphysics coupling algorithm has been developed based on open-source SALOME platform. MED data structure and HDF5 functions have been used for all the field operations. The coupled system is solved for different computational cases: laminar natural circulation, turbulent $k - \omega$ with SUPG regularization and with standard up-wind regularization for the advection term. Each case is also simulated through two different heat exchange models: with constant and non constant turbulent Prandtl number. These tests show the importance of the coupling approach for the analysis of transient simulations where the three-dimensional phenomena play an important role.

1 INTRODUCTION

Nowadays generation IV reactor designs are studied in order to achieve low probability of core damage and to reduce the risk of the fission product release to the environment. This goal is reached also thanks to the passive safety features, such as passive residual heat removal systems. For this purpose there is an increasing interest in efficient and accurate tools for thermal-hydraulic numerical simulations and safety analysis of these reactors. These simulations are very challenging due to the new materials used for the primary loop and to the high complexity of these systems. Since Computational Fluid Dynamics (CFD)

codes are computationally too expensive for resolving the whole primary coolant system of a reactor, and one-dimensional system codes are generally inadequate for resolving complex transients with mixing and stratification, a coupling algorithm is introduced in order to correct iteratively a system code's solution through the CFD simulation of one or more components of the circuit. The momentum and energy conservation equations are solved into the CFD code for different computational cases: laminar natural circulation, turbulent $k - \omega$ with SUPG regularization and with standard up-wind regularization for the advection term. The coupling algorithm is tested on the numerical simulation of the evolution of an unprotected loss of flow going from forced to natural circulation flow in the experimental TALL-3D facility. TALL-3D is a liquid Lead Bismuth Eutectic loop with an oil-cooled secondary loop, developed at KTH (Royal Institute of Technology, Stockholm, Sweden) as part of the EU THINS project. It was designed in order to provide mutual feedback between natural circulation in the loop and complex 3D mixing and stratification phenomena in a pool-type test section, and to give the possibility to validate standalone system and CFD codes for each subsection of the facility [1, 2]. The goal of this paper is to develop computational multiscale algorithms with the purpose of studying issues of LFR technology. The coupling on the platform is performed between the system code CATHARE 2 and the finite-element based in-house code FEMuS by an algorithm based on the overlapping domain method. Interested reader on overlapping method can see [3, 4, 5, 6, 7]. The results of the coupled numerical simulation are compared with the experimental results, in order to validate the used codes and the presented coupling algorithm for nuclear power safety analysis.

2 NUMERICAL MODELING

In this section a brief description of the TALL-3D experimental setup is presented, together with a brief description of the instrumentation for the measurements of the tested physical properties. Numerical modeling of the one-dimensional circuit with a system code is introduced, and the physical and numerical models for the CFD simulations into the 3D test section are then presented.

2.1 Experimental setup

TALL-3D facility operates with Lead-Bismuth Eutectic (LBE, melting point 125°C). It incorporates a main LBE loop, a secondary cooling side and a differential pressure measurement system. The primary loop consists of the sump tank used to store, melt and supply lead-bismuth into the main loop, 3 vertical legs (named *Main Heater*, *3D* and *Heat Exchanger* leg) and 2 connecting horizontal sections each combining 2 elbows and a T-junction. Total electric power is about 80 kW. The Main Heater leg is composed by a 27 kW electric heater and an expansion tank on the top. The Heat Exchanger leg has a counter-current heat exchanger at the top and the circulation pump at the bottom. The 3D leg connect the 3D test section, where the CFD simulations will be performed, to the loop. The secondary loop utilizes Dowtherm RP heat transfer fluid in order to control heat balance in the primary loop.

The 3D test section is an axisymmetric cylindrical stainless steel vessel. The inlet of the fluid is at the bottom and the outlet at the top of the vessel. The upper two-thirds of the test section is equipped with a 15 kW heater installed around the whole circumference. Inside the test section, a circular plate is placed perpendicularly to the flow direction in order to increase pool mixing by deflecting the inlet flow to periphery. The decrease of the flow rate inside the 3D leg, together with the installed heater, promotes development of thermal stratification in the LBE pool.

The validation of coupled codes is carried out thanks to a set of data given by measurement system. The main loop is equipped in order to provide necessary boundary conditions on inlet and outlet LBE temperatures, pressure difference over the section and LBE mass flow rate. For the comparison between the experimental data and the simulated results, LBE temperature is measured at 25 locations around the main loop piping, and 154 thermocouples are provided for measurements in the 3D test section. A differential pressure measurement system is provided in order to evaluate pressure drop on 7 connected subdomains, providing a complete coverage of the loop. The LBE mass flow rate is measured by two flow meters located on Heat Exchanger and 3D legs; mass flow rate in the Main Heater leg is estimated by mass conservation. For further information on TALL-3D experimental setup, physical data, instrumentation and measurements one can see [1].

2.2 Thermohydraulic system code model

CATHARE 2 is used as one-dimensional system code (shown in Figure 1 on the left). In the previous section a brief description of each leg has been carried out. The central vertical leg (3D leg) is the key part of the circuit since it contains the 3D test section. It consists of three AXIALS: the ABOVE3D, BELOW3D and 3DPIPE module. As one can see in Figure 1 on the right we consider six reference points labeled by $S1$, $S2$, $S3$, $S4$, $S5$ and $S6$. The points $S1$ and $S2$ are located along the Main Heater (left) leg. The point $S1$ is in the COR module, the point $S2$ is inside the RESERVE module. We denote such points with COR3 and RESERVE4, respectively. The points $S3$ and $S4$ are located in the 3D (central) leg. The point $S3$ is in the BELOW3D module, the point $S4$ is inside the ABOVE3D module. We denote such points with BELOW3D24 and ABOVE3D8. Finally the points $S5$ and $S6$ are located along the Heat Exchanger (right) leg. The point $S5$ is in the LINUP2 module and the point $S6$ is in the PUMP module. In a similar way we denote such points with LINUP14 and PUMP.

The top horizontal part of the LBE circuit (shown in the top part of Figure 1) consists of the main expansion tank (labeled with TANK), two AXIALS (LINUP1, LINUP2) and a volume which links this part of the top LBE circuit to the 3D leg with the three-dimensional test section. The TANK volume and the LINUP2 are connected with the Main Heater and Heat Exchanger leg, respectively. The bottom horizontal part of the LBE circuit (shown in Figure 1 on the bottom) consists of 2 axial modules (LINDOWN, DOWNPUMP) and a volume module (VOLDDOWN) which links the bottom to the 3D leg with the three-dimensional test section. For further information on CATHARE system code one can see [8, 9, 10].

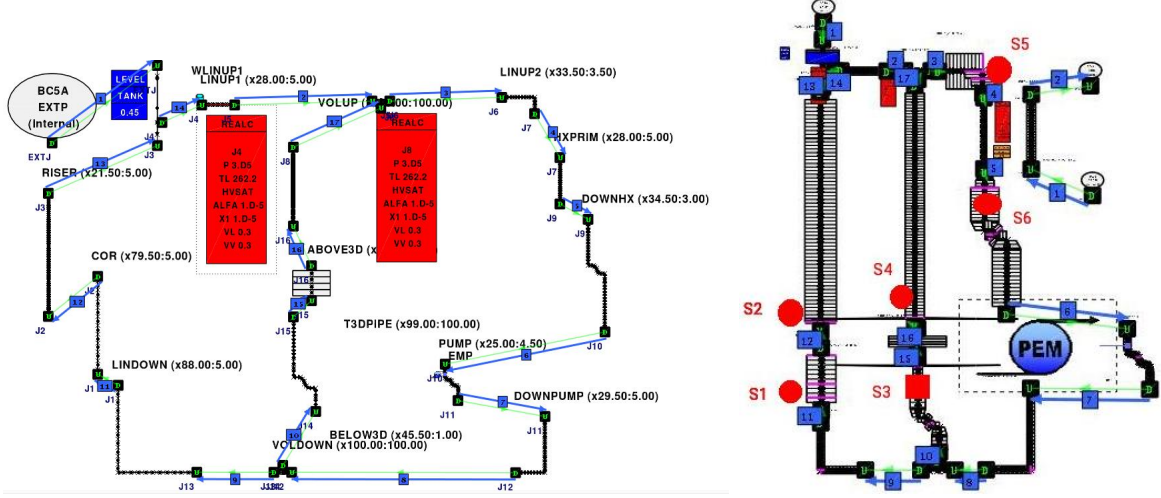


Figure 1: CATHARE model for the TALL-3D facility (left) and point of interests (right) $S1-S2$ of the Main Heater leg, $S3-S4$ of the 3D leg and $S5-S6$ of the Heat Exchanger leg.

2.3 CFD model

Momentum conservation equations. For three-dimensional simulations we use a finite element open-source code able to solve multiphysical problem. The TALL-3D test section is solved for different computational cases, including laminar natural circulation and turbulent $k - \omega$. Let (\mathbf{u}, p) be the state of the fluid flow that enters into the studied domain, defined by the velocity and pressure solution of the Navier-Stokes equations. Let us consider an incompressible fluid, with density slightly variable as a function of temperature $\rho = \rho(T)$. For high Reynolds numbers (Re) the turbulence model can be defined by splitting the velocity vector into a resolved-scale field $\bar{\mathbf{u}}$ and a subgrid-scale field $\bar{\mathbf{u}}'$. By substituting $\mathbf{u} = \bar{\mathbf{u}} + \bar{\mathbf{u}}'$ and $p = \bar{p} + p'$ in the incompressible Navier-Stokes equations and then filtering the resulting equation, the equations of motion for the average fields $\bar{\mathbf{u}}$ and \bar{p} are

$$\nabla \cdot (\mathbf{u}) = 0, \quad (1)$$

$$\rho \frac{\partial \mathbf{u}}{\partial t} + \rho (\mathbf{u} \cdot \nabla) \mathbf{u} = -\nabla p + \nabla \cdot [\mu (\nabla \cdot \mathbf{u} + \nabla \cdot \mathbf{u}^T) - \rho \overline{\mathbf{u}' \mathbf{u}'}] + \rho \mathbf{g}. \quad (2)$$

In (1), (2) and in the following, \mathbf{u} and p are the mean velocity and mean pressure. The unknown Reynolds stresses $\rho \overline{\mathbf{u}' \mathbf{u}'}$ are modeled with the $\kappa - \omega$ model in order to close the Navier-Stokes system.

In the $\kappa - \omega$ model, where κ is the turbulent kinetic energy and ω the specific dissipation rate, the turbulent viscosity μ_t is defined as $\mu_t = \rho \kappa / \omega$. The standard $\kappa - \omega$ system is defined by

$$\frac{\partial \rho \kappa}{\partial t} + \nabla \cdot \rho \mathbf{u} \kappa = \nabla \cdot \left[\left(\frac{\mu_t}{\sigma_k} + \mu \right) \nabla \kappa \right] - \rho \beta_k \kappa \omega + \rho \gamma_k S^2, \quad (3)$$

$$\frac{\partial \rho \omega}{\partial t} + \nabla \cdot \rho \mathbf{u} \omega = \nabla \cdot \left[\left(\frac{\mu_t}{\sigma_w} + \mu \right) \nabla \omega \right] - \rho \beta_w \omega^2 + \rho \gamma_w S^2, \quad (4)$$

with $\beta_k = 9/100$, $\gamma_k = \mu_t$, $\beta_w = 5/9$, $\gamma_w = 3/40$, $\sigma_k = 2$ and $\sigma_w = 2$. S is the modulus of the mean rate-of-strain tensor, defined as

$$S \equiv \sqrt{2S_{ij}S_{ij}} = \frac{1}{2}\|\nabla\mathbf{u} + \nabla\mathbf{u}^T\|. \quad (5)$$

Energy conservation equations. The evolution of the system is described by the solution $e = e(T, \mathbf{u})$, where e represents the total energy $e \equiv C_v T + \frac{\mathbf{u}^2}{2}$, of the following equation

$$\frac{\partial \rho e}{\partial t} + \nabla \cdot (\rho \mathbf{u} e) = \Phi + \nabla \cdot \mathbf{q} + \dot{Q}. \quad (6)$$

The heat flux, \mathbf{q} , is given by Fourier's law $\mathbf{q} = -\lambda \nabla T = -C_p \frac{\mu}{Pr} \nabla T$. The laminar Prandtl Pr is defined by $Pr = \frac{C_p \mu}{\lambda}$. The fluid can be considered incompressible and the density slightly variable as a function of temperature $\rho(T) = a + \gamma T$, where a and γ are constants. The quantity \dot{Q} is the volume heat source and Φ the dissipative heat term. C_v is the volume specific heat. The equation is completed with appropriate boundary conditions.

For high Reynolds numbers again we decompose the velocity and temperature fields into a resolved scale field and a subgrid-scale field. With usual notation these approximation models result in the same equations as (6) for the average fields ($T = \bar{T}$) and in a modified heat flux \mathbf{q} as follows

$$\mathbf{q} = -C_p \left(\frac{\mu}{Pr} + \frac{\rho \nu_t}{Pr_t} \right) \nabla T. \quad (7)$$

The computation of the turbulent Prandtl number Pr_t determines the turbulence contribution. Two models have been implemented: the constant turbulent Prandtl number model and the κ - ϵ - κ_t - ϵ_t turbulence model. The second one is still in progress and it is available only for development studies. For many fluids Pr_t can be assumed to be constant, and its values range from 0.85 to 0.95. In a more advanced model the turbulent Prandtl number may be defined as

$$Pr_t = Pr_{t0} [B(\nu, \nu_t, Pr, R) + 1] C_\alpha \frac{R + C_\gamma}{2R}, \quad (8)$$

where $R = \kappa_t \epsilon / \epsilon_t \kappa$ and C_α, C_γ are constants. The function $B(\nu, \nu_t, Pr, R)$ can take several forms. The equation for the *averaged temperature squared fluctuations* is defined by the following transport equation [11]

$$\frac{\partial \kappa_t}{\partial t} + \mathbf{u} \cdot \nabla \kappa_t = \nabla \cdot \left[\left(\alpha + \frac{\alpha_t}{\sigma_{\kappa_t}} \right) \nabla \kappa_t \right] + P_t - \epsilon_t, \quad (9)$$

where

$$P_t := -\overline{\mathbf{u}'T'} \nabla T = \frac{\nu_t}{Pr_t} (\nabla T)^2. \quad (10)$$

In a similar way an equation for ϵ_t can be written as [11]

$$\frac{\partial \epsilon_t}{\partial t} + \mathbf{u} \cdot \nabla \epsilon_t = \nabla \cdot \left[\left(\alpha + \frac{\alpha_t}{\sigma_{\epsilon_t}} \right) \nabla \epsilon_t \right] + \frac{\epsilon_t}{\kappa_t} \left(C_{p1} P_t - C_{d1} \epsilon_t \right) + \frac{\epsilon_t}{\kappa} \left(C_{d1} P_k - C_{d2} \epsilon \right), \quad (11)$$

where P_k is defined by

$$P_k := -\overline{u'_i u'_j} \frac{\partial u_i}{\partial x_j} = \nu_t \left(\frac{\partial u_i}{\partial x_j} + \frac{\partial u_j}{\partial x_i} \right) \frac{\partial u_i}{\partial x_j}. \quad (12)$$

The coefficients can be considered as constants, with values $C_{p1} = 1$, $C_{p2} = 0.60$, $C_{d1} = 1$ and $C_{d2} = 0.9$ or as model functions. The coefficient α_t is the thermal expansion coefficient. An approximation of this model can be obtained by assuming the Kays approximation $Pr_t = 0.85 + 1.5(1 + \nu_t/Pr)^{-1}$.

The presented momentum and energy equations are implemented on FEMuS together with the turbulence models, and some test cases are up-winded with a SUPG formulation [12]. For details on the adopted turbulence model one can refer to [11, 13, 14, 15].

3 COUPLING ALGORITHM

In this work the platform SALOME is used for the integration of external numerical codes to produce a new application with full pre and post processing management of CAD models. The integration of a code on the SALOME platform is obtained by generating an interface with functions available in the MEDMem library (based on MED data format) that allows the data transfer from the platform to the code and vice versa [5]. The CATHARE system code have been developed with an interface on SALOME platform for coupling and integration. The coupling procedure can be divided into 3 main steps: generating the mesh duplicate in the MED format, handling the solution in the data structure and imposing the solution on the target code. Customized C++ routines are designed for the data transfer for each code which can compute field mean integral values using Gauss integration and point wise field interpolations. These routines work on MED data format and can be used with all the numerical codes where this format has been adopted for input/output and mesh storage data.

An overlapping domain method is implemented for the coupling between CFD and system code [16]. The one-dimensional mesh is defined over all the domain and a three-dimensional mesh is defined only in the 3D test section. Inlet boundary conditions for the 3D test section are obtained from the corresponding fields on CATHARE code, thanks to the imposition of an uniform flat profile equal to the field's value on the corresponding CATHARE mesh element. At the point S3 (Figure 1) the liquid flow and temperature values of the one-dimensional code are imposed as inlet boundary conditions in CFD code.

The feedback of CFD on system code is obtained with an algorithm based on the defective method [4], [6]. Since the mesh are overlapping, and no flow may exit from the test section there can be no error in the mass balance equation. A brief description of defective method is now introduced. Let us consider λ as a generic variable whose system code solution can be improved with the CFD one. We label with λ_{1D} and λ_{CFD} the values of λ from the system and the CFD code. λ_{CFD} is calculated as a mean integral value. The defective method is based on an iterative correction of the system code by the imposition of fictitious source terms (at generic time step n) \mathcal{S}^n , calculated as

$$\mathcal{S}^n = \mathcal{S}^{n-1} - \omega_\lambda (\lambda_{CFD} - \lambda_{1D}), \quad (13)$$

where ω_λ is an under relaxation parameter smaller than 1. In this way, the solution of the system code λ_{1D} is corrected with the mean value of the 3D solution λ_{3D} , and no correction is imposed when $\lambda_{1D} = \lambda_{3D}$. In this work λ can be the pressure loss across the CFD domain and across the overlapping mono-dimensional domain or the temperature on boundary interfaces.

The energy correction is obtained by an heat flux $\mathcal{S}^n = h_{1D}^n$, by computing $h_{1D}^n = h_{1D}^{n-1} - \omega_{ex} C_p (T_{1D} - T_{3D})$, where all values are referred to the outlet section (point S4 in Figure 1 on the right) of the CATHARE and CFD code. CATHARE values are labeled with $1D$ and CFD code values are labeled as $3D$. T_{3D} is the average temperature at the outlet of the 3D test section, which has been computed after the FEMuS time step. The momentum correction is obtained by computing the a pressure source term $\mathcal{S}^n = DPLEXT_{1D}^n$ as $DPLEXT_{1D}^n = DPLEXT_{1D}^{n-1} - \omega_p (\Delta p_{3D} - \Delta p_{1D})$, where Δp_{3D} and Δp_{1D} are the pressure losses, when the gravity contribution is subtracted, of the three- and one-dimensional 3D test section, respectively. Under relaxation parameters ω_{ex} and ω_p are set to 0.1 [3].

4 RESULTS

Results of numerical simulation of the TALL-3D multiscale model are presented in this section. In order to set the initial conditions to the one-dimensional system code, a steady state solution of the mono-dimensional model is computed.

CATHARE standalone simulations. The evolution of an Unprotected Loss of Flow, which reproduces a forced to natural transient, is considered. At first a CATHARE standalone simulation has been carried out. The initial conditions imposed on some point of interest (see Figure 1) are reported in Table 1.

Table 1: Initial state condition that satisfies the steady state equation.

	Initial Condition	Unit
T BELOW3D	241.45	$^{\circ}C$
T ABOVE3D	259.81	$^{\circ}C$
T LINUP2	251.76	$^{\circ}C$
T PUMP	242.38	$^{\circ}C$
T COR	244.16	$^{\circ}C$
T RESERVE	248.33	$^{\circ}C$
MH rod power	2578	W
3D vessel power	4833	W
LBE mass flowrate	4.2750	kg/s

Experimental data are provided in [1, 17, 18]. In Figure 2a) results of the mass flowrate in the 3 legs are reported, both for CATHARE-alone simulation and experimental results. In the following, FM1 and TC1 measures will refer to the Heat Exchanger leg, FM2 and TC2 to the 3D leg and FM3 and TC3 to the Main Heater leg. From Figure 2b) to 2d) temperature at thermocouple points, located the circuit, are compared with the temperature

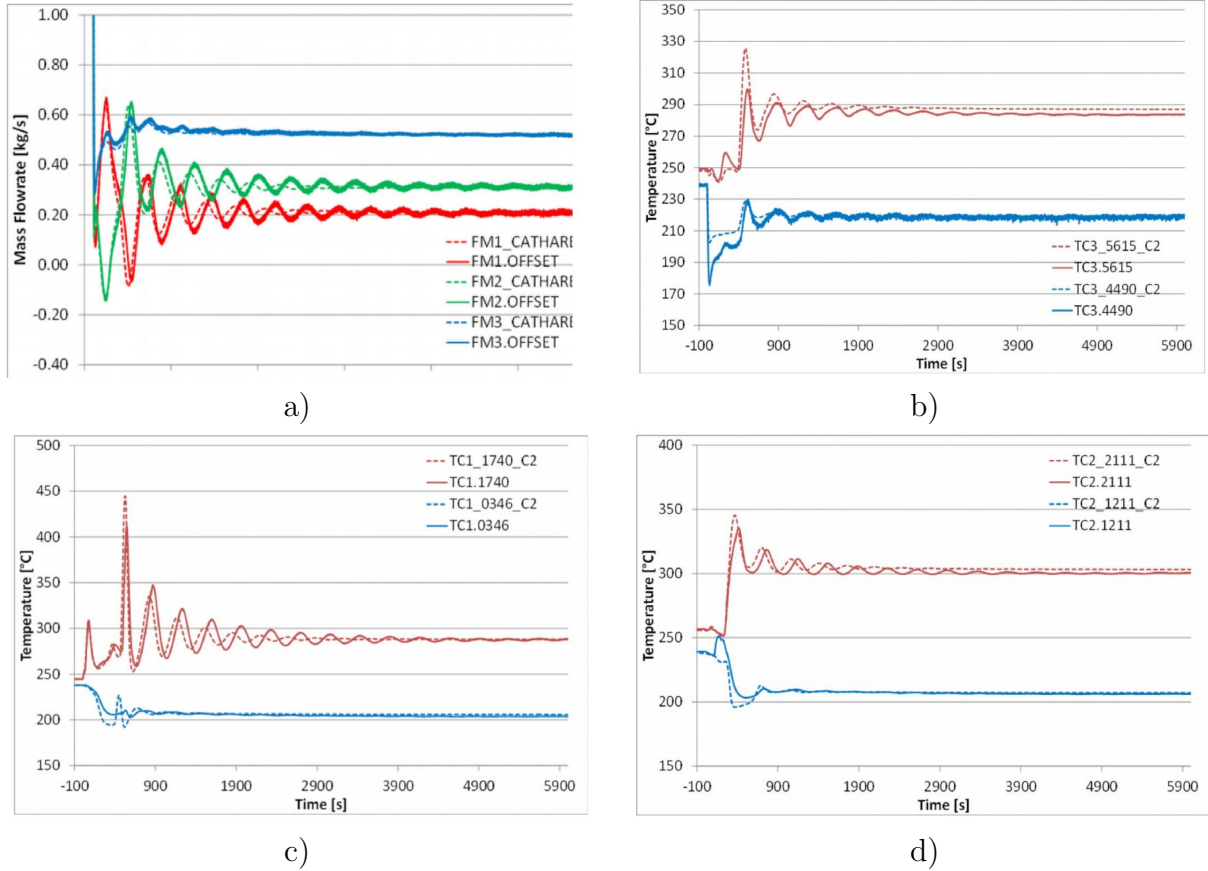


Figure 2: Comparison between experimental (continuous lines) and computational CATHARE standalone simulations (dotted lines). Mass flowrate comparison in a). Temperature comparison in: b) Main Heater leg, c) Heater Exchanger leg, d) 3D leg.

at matching points of CATHARE model. In particular, two thermocouples are considered for each leg. The “_C2” suffix represents a label for CATHARE measurements. The magnitude and frequency of the external mass flow rate oscillations are well captured, but differences between the simulations and experimental data can be observed. During the initial transient phase, even though the thermal balances are reliable only in steady-state conditions, a discrepancy of the heat exchanging condition is observed. The facility heat losses during the transient are almost constant at about $2.2kW$. The lower heat exchange affects the temperature evolution as can be seen in the pictures 2 b)-d). The experimental inlet temperature increases during the reverse flow phase due to mixing effects in 3D vessel. This behavior cannot be caught by system codes.

Coupled simulation results. In Figure 3 on the left the geometry of simulated 3D test section is shown. It is also reported, on the right, the velocity modulus inside the 3D test section in one of the studied cases (laminar flow, $t = 1000s$). The solutions of coupled system are then reported for different computational cases: laminar natural circulation (case A and B), turbulent $k - \omega$ with SUPG regularization (case B, C and

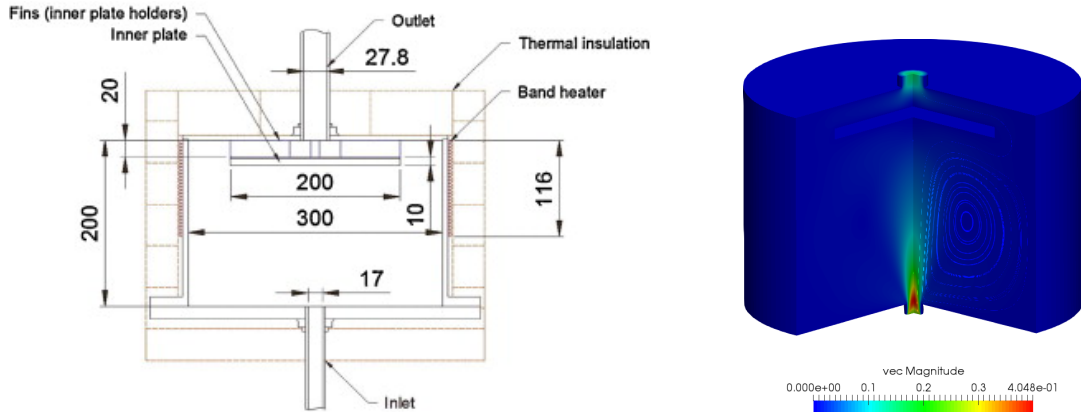


Figure 3: Geometry and dimensions of the 3D test section (left), modulus of the velocity field (with streamlines) inside the 3D test section (right).

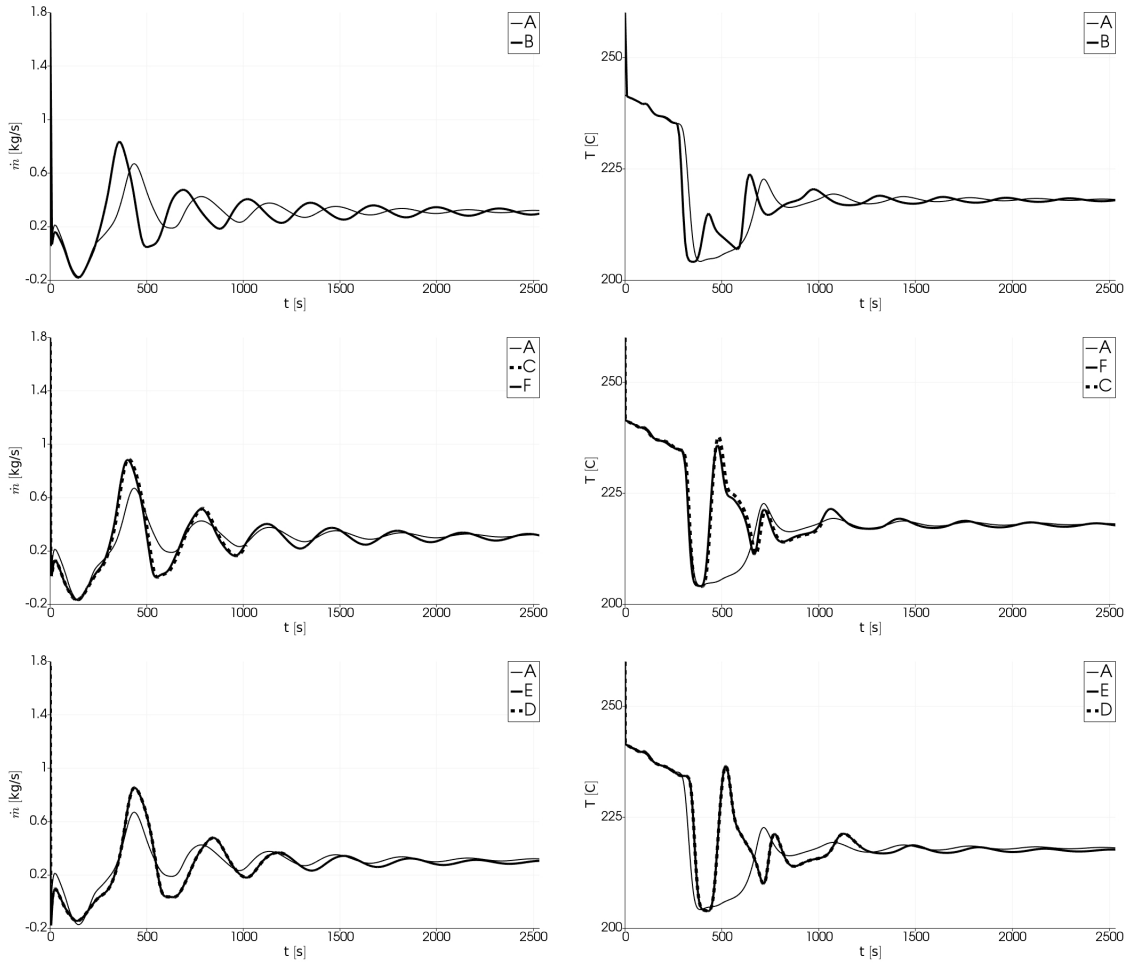


Figure 4: Numerical results at point S3 (BELOW3D, 3D leg) of mass flow (left) and temperature (right) for cases AB, ACF and ADE (from top to bottom).

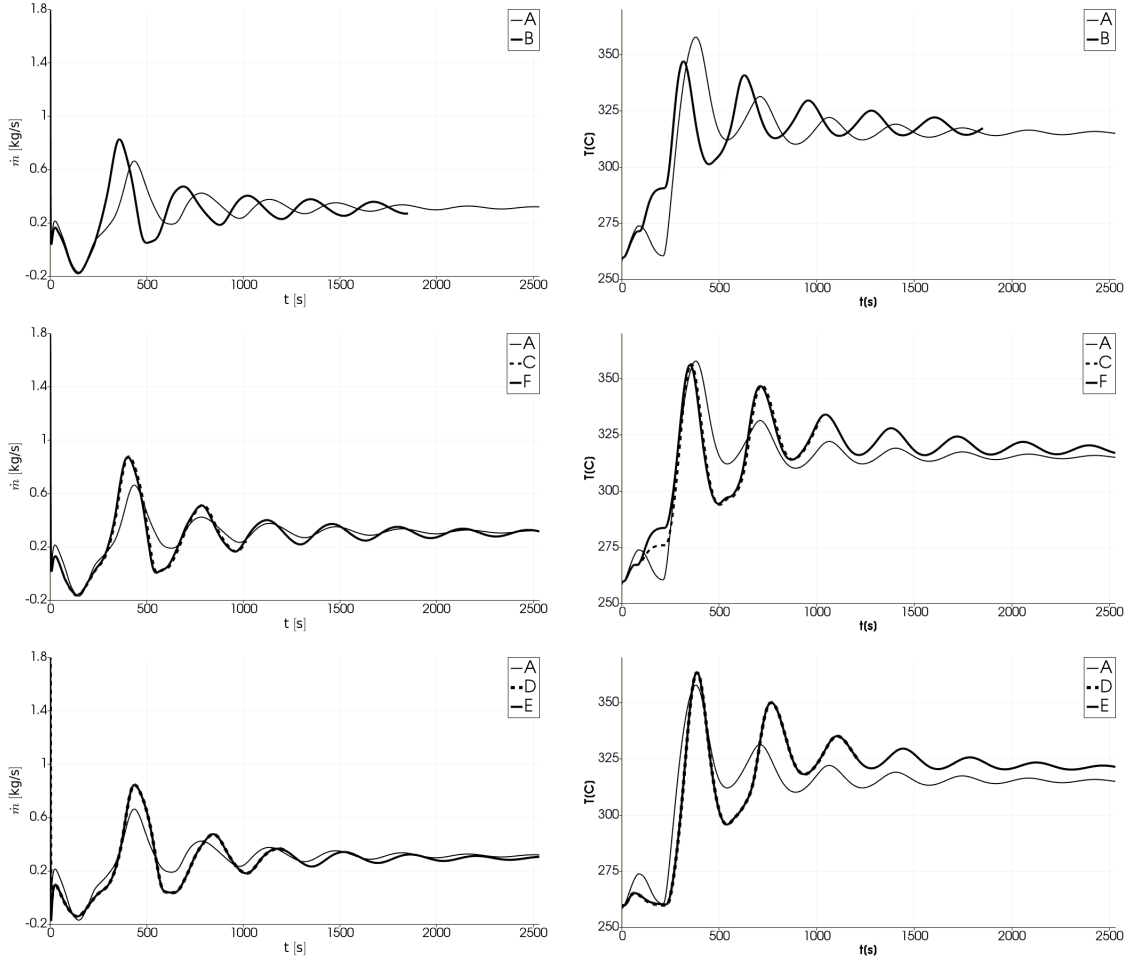


Figure 5: Numerical results at point S4 (ABOVE3D, 3D leg) of mass flow (left) and temperature (right) or cases AB, ACF and ADE (from top to bottom).

F) and standard upwind regularization (case D and E) for the advection term. Inside each case two different turbulent heat exchange models are used. In cases C and D a constant turbulent Prandtl number is considered, so the turbulent thermal diffusivity is proportional to the turbulent viscosity. In cases E and F a variable Prandtl number is used, as discussed in section 2.3. In Table 2 all the tested cases are summarized.

Table 2: Models used for all the simulated cases. Case A refers to CATHARE standalone.

	A	B	C	D	E	F
Stabilization	-	SUPG	SUPG	Upwind	Upwind	SUPG
Dynamic Turbulence model	-	-	$k - \omega$	$k - \omega$	$k - \omega$	$k - \omega$
Thermal Turbulence model	-	-	Constant Pr_t	Constant Pr_t	Kays Pr_t	Kays Pr_t

In Figures 4 and 5 numerical results of mass flow rate (on the left) and temperature (on the right) are presented for the 3D test section's inlet and outlet, respectively. Results

of cases from B to F are obtained from CATHARE simulation, corrected iteratively with the CFD results thanks to the defective method, as described in section 3. We compare the coupled computation with the uncoupled one by keeping the case A in all the Figures. In Figure 4 a comparison between CATHARE standalone simulation A and CFD laminar case B is presented on the top. In the middle, the turbulent cases C and F with SUPG regularization are compared. On the bottom, case D and E are then reported. The differences between SUPG and Upwind regularization are negligible, and also differences between a constant or a variable Prandtl number. Differences can be observed between turbulent cases and laminar case B. Furthermore, CATHARE standalone simulation differs from all the computed simulations. Results on the outlet of the test section, in Figure 5, has similar behavior. Some differences are registered between cases C and D, so the outlet temperature of 3D test section is affected by the used regularization method.

However the dynamic coupling between a one-dimensional code and a three-dimensional one with a turbulent model leads to complex problems since the turbulent quantities should be passed as boundary conditions. The one-dimensional flow does not have dimensionality and the dimensional turbulence effects are not taken into account in a very accurate way. The turbulence kinetic energy and its rate at the boundary are fundamental and therefore it is necessary to develop appropriate models that can lead to improved coupling. The use of this model in a trivial manner can give even to less accurate simulations than the standalone case.

5 CONCLUSIONS

In the present work a computational platform based on open-source SALOME software is developed with the purpose of studying issues in LFR technology. The platform is able to couple research in-house code FEMuS with system code CATHARE. The data exchange between different codes requires the creation of interfaces that are used to read and manipulate code solutions. MED data format, that comes with the MEDmem libraries, is used for the creation of these interfaces. Thanks to the MEDmem libraries and their HDF5 functions, the coupling operations are performed within the computer memory allowing good numerical code coupling performance. TALL-3D experimental facility has been simulated in order to validate and evaluate the performance of this coupling method. During the analysis of this lead-cooled facility three-dimensional effects cannot be ignored and its features cannot be modeled by simple balances of energy, momentum and mass. The use of laminar flow to model the three-dimensional components gives good results. However the introduction of turbulence models has not increased the matching with experimental results showing that the turbulence boundary conditions taken from the one-dimensional circuit need to be enforced correctly by modeling appropriately such a coupling. The proposed algorithm, validated to perform multiscale computations, shows good performance and can be seen as a valid tool to improve system code standalone simulations. However, further work is necessary for a complete validation of turbulence multiscale simulations for this facility.

ACKNOWLEDGEMENT

The authors gratefully acknowledge the Managing Board of ECCOMAS for the scholarship covering the full registration to the Congress and the support travel and accommodation expenses.

REFERENCES

- [1] Grishchenko D, Jeltsov M, Kööp K, Karbojian A, Villanueva W, and Kudinov P 2015 *Nuclear Engineering and Design*, **290** 144-153.
- [2] Pacio J, et al. 2015 *Nucl. Eng. Des.* **290** 27-39
- [3] Chierici A, Chirco L, Da Vià R, Manservisi S, and Scardovelli S. 2017 *Journal of Physics: Conference Series* Vol. **923**, No. 1.
- [4] Grunloh T P and Manera A 2016 *Annals of Nuclear Energy* **90** 422-32.
- [5] D. Cerroni *Multiscale multiphysics coupling on a finite element platform*, Ph.D. thesis University of Bologna (2016).
- [6] Bavière R, Tauveron N, Perdu F, Garré E and Li S 2014 *Nucl. Eng. Des.* **277** 124-37
- [7] Tenchine D et al. 2012 *Nucl. Eng. Des.* **245** 14052.
- [8] Bestion D 1990 *Nuclear Engineering and Design* **124.3**: 229-245.
- [9] Barre F and Bernard M 1990 *Nuclear engineering and design* **124.3**: 257-284.
- [10] Robert M, et al. "CATHARE 2 v2. 5: a fully validated CATHARE version for various applications." 2003.
- [11] Da Vià R, et al. 2016 *Int. J. of Heat and Mass Transfer* **101** 1030-1041
- [12] Bochev P B, Gunzburger M D and Shadid J N 2004 *Comput. Methods in Appl. Mech. Eng.* **193** 2301-23
- [13] Ilinca F, Hetu J F and Pelletier D 1998 *Computers and Fluids* **27** 291-310
- [14] Manservisi S and Menghini F 2014 *Int. J. Heat Mass Tran.* **69** 312-26
- [15] Manservisi S and Menghini F 2014 *Nucl. Eng. Des.* **273** 251-70.
- [16] Aulisa E, et al. 2009 *Communications in Computational Physics* **6(2)** 319-341
- [17] Grishchenko D, et al. 2012 *Proc. of The 9th Int. Top. Meeting on Nuclear Thermal-Hydraulics, Operation and Safety (NUTHOS-9)*, N9P0299, 2012.
- [18] Grishchenko D, et al. 2014 *THINS International Workshop Modena, Italy*.